JOURNAL OF THERMOPHYSICS AND HEAT TRANSFER
Vol. 22, No. 1, January–March 2008

Experimental Investigation of New Flat-Plate-Type Capillary Pumped Loop

Zhichun Liu,* Wei Liu,† and Jinguo Yang‡
Huazhong University of Science and Technology, 430074 Wuhan, People's Republic of China

DOI: 10.2514/1.31746

A capillary pumped loop is a two-phase heat transfer device which has been increasingly applied in thermal control of satellite or spacecraft and electronic cooling. However, startup performance of a normal capillary pumped loop is poor and hydrodynamic oscillation in the system appears sometime during its operation. A flat-plate-type capillary pumped loop is constructed and tested in the present study, which combines the advantages of a capillary pumped loop and a loop heat pipe by improving both system and components. In the present capillary pumped loop, both evaporator and condenser are designed as a type of flat plate with porous wick, and a reservoir is used to control and adjust operation temperature of the system. In addition, a subcooler is adopted to improve the quality of working fluid flowing back to the evaporator. A plane type of evaporator with a cross channel for the liquid supply was made to reduce the probability of a dry-out point caused by strong evaporation in the case of high heat flux, and therefore to enhance the stability of the system. Also, a plane type of condenser with a porous wick is designed, which is of the three ports for vapor-pipe inlet, liquid-pipe outlet, and an adjusting pipe connected to a reservoir. The startup performance of the system benefits greatly from this three-port design, as liquid in the system can be easily pressed into a reservoir due to resistance reduction. The performance of a capillary pumped loop prototype was tested in startup, persistence operations, and different vacuum. Startup experiments under different heat loads and working conditions were conducted. Excellent startup performance, being stable and easy, has been shown for the plane-type capillary pumped loop system, which validates the new configuration. Pressure oscillation and temperature fluctuation in the system were reduced largely owing to the induction of a porous wick in the plane condenser. During experimental processes lasting more than 10 h, the new type capillary pumped loop shows outstanding thermal behavior and no dry-out phenomena were observed. The testing results indicate that 1) the new capillary pumped loop system shows excellent startup performance without pressure priming and liquid clearing of vapor line; and 2) the new capillary pumped loop system is stable under very severe operational conditions, such as low load, sudden power step, etc.

I. Introduction

WITH the continuous increasing of applied heat load in current and future satellite or spacecraft systems, waste heat dissipation in these systems becomes a more and more challenging job for thermal scientists. The new means or technologies for heat dissipation with high efficiency are strongly needed. Two-phase heat transfer devices with capillary pumping are of particular interest in spacecraft applications because of their high thermal capacity and long distance heat transfer ability. A capillary pumped loop (CPL) is one of these advanced two-phase thermal control devices which uses the phase change to transfer heat and allows heat transport at nearly constant temperature. The main components of a typical CPL include evaporator, condenser, reservoir, and vapor/liquid pipeline. During normal operation of a CPL, heat is first applied to the evaporator to cause the working fluid to evaporate. Then the evaporation vapor carries the heat through the vapor pipeline to the condenser where the vapor is condensed, the thermal energy in vapor is released, and removed by the heat sink. The condensed fluid in the condenser goes back to the evaporator by the capillary pumping force created by the capillary evaporator and another thermal and flow cycle starts. It is noted that the operation parameters in the CPL reservoir such as temperature and pressure determine the loop pressure and saturation temperature in total CPL.

The concept of CPL was first presented by Stenger of NASA John H. Glenn Research Center at Lewis Field in 1966 [1]. At that time, it did not receive significant attention until the late 1970s, when the situation greatly changed. Up to now, CPLs have been under intensive investigation for space application and electronic device cooling in many countries [2–5]. A lot of CPLs have been designed and fabricated, and ground tests for these CPLs are conducted. Several designs are even tested in flight experiments and some of them have been applied in real spacecraft thermal management [2,4]. Despite the flourishing development of a CPL, there are still some problems that plague the applications of CPL, such as startup difficulty and not being robust and reliable due to pressure oscillation during CPL operation. To solve or partly solve the above problems, a CPL needs preconditioning to ensure that the wick is wetted before applying power to the evaporator for startup. This involves the reservoir preheating to "prime" the evaporator pump and collapse any vapor bubbles, and this process is tedious and sometimes time consuming [6,7]. Once the priming procedure is completed, the heat can be applied to the capillary evaporator to start the loop operation, and this startup procedure is called "fully flooded startup." When the evaporation commences, vapor generated by the evaporator must displace the liquid in the vapor line with the same volumetric flow rate with which it moves to the reservoir. The above process can cause the largest liquid velocities that the CPL will ever encounter, and most of the liquid with large velocity must pass through nearly all of the CPL pipeline to arrive in the reservoir. When the pressure difference required to perform this purge exceeds the capillary limit of the wick, vapor bubbles from the vapor side will certainly be injected through the wick into the liquid core and cause depriming, which is responsible for more than 90% of CPL depriming [8]. To

Received 22 April 2007; revision received 4 September 2007; accepted for publication 15 September 2007.

*Assistant Professor, School of Energy and Power Engineering; zcliuqd@163.com.
†Professor, School of Energy and Power Engineering; w_liu@hust.edu.cn (Corresponding Author).
‡Associate Professor, School of Energy and Power Engineering.

enhance the possibility of startup success, the CPL system generally uses starter heaters and a starter pump for clearing liquid in the vapor line; nevertheless, sometimes the CPL still cannot start up successfully [6,7].

The pressure oscillation is another issue of concern and has been intensively investigated due to its deleterious effects on CPL operation [9–11]. To reduce CPL pressure and temperature fluctuations, a condenser with a porous element was proposed by Muraoka [10], who performed theoretical and experimental studies. The results showed that these structures can reduce, even eliminate the pressure oscillations, and greatly improve the operational performance of the CPL. Qu et al. [7] conducted an analytical investigation to understand the internal fluid flow and heat transfer in the condenser with porous wick of a CPL system. A mathematical model is proposed and used to describe the flow and heat transfer, especially interfacial transport phenomena. The liquid–vapor interface of the condensed liquid film was numerically determined. Some factors, such as vapor pressure, wall subcooling, wall heat load, and thermofluid properties, have significant influence on the heat transfer process and the shape of the liquid–vapor interface. Meanwhile, an experimental facility was set up and an experimental investigation was completed. Theoretical prediction and experimental results show quite good consistence. However, their CPL system has no reservoir, which causes the poor thermal controlling capability. Huang and Liu [12,13] performed theoretical analysis and a numerical study of the phase-change heat transfer in the porous wick of the CPL evaporator which is similar to Muraoka's.

Liao and Zhao [14] conducted an experimental investigation of capillary-driven heat and mass transfer in a vertical rectangular capillary porous structure heated from a grooved block placed on the top. The experimental results show that with an increase of the imposed heat flux, the heat transfer coefficient increases to a maximum value and then decreases afterward. In their paper, the heat transfer mechanisms leading to the maximum heat transfer coefficient and the critical heat flux are explained based on the visual observation of the phase-change behavior and the measured temperature distributions within the porous structure. Figus et al. [15] conducted a numerical investigation of heat and mass transfer within a porous structure with partial heating and vaporization on the upper surface, and the results indicate that capillary fingering may limit the operating range of CPL.

A loop heat pipe (LHP) is also a vaporization/condensation phase-change heat transfer device which also uses surface tension force created by the evaporator wick to drive the fluid circulation. In a LHP, the compensation chamber is made as an integral part of the evaporator and is directly connected to the evaporator by a secondary wick. In addition, the compensation chamber (CC) is located directly in the path of the liquid flow. These differences with CPL allow the LHP to realize an easy startup process and robust operation, but the heat leak through the secondary wick to the CC makes controlling the loop temperature difficult [6].

The objective for the present study is to design, build, and test a new type of CPL. It has a flat-plate type evaporator and a condenser with a capillary wick. The present design aims to realize the quick startup without pressure priming and liquid clearing in the vapor line as well as a stable operation at different conditions.

II. CPL Design and Experimental Setup

The CPL design is related to the maximum capillary pressure created by the wick structure and working fluid. The maximum capillary pressure can be calculated by the Young–Laplace equation

$$(\Delta P_c)_{\max} = \frac{2\sigma}{r_{\text{eff}}} \tag{1}$$

where σ is the coefficient of surface tension, and r_{eff} is the effective radius of the capillary.

Based on a fundamental principle to the CPL operation, the maximum capillary pumping head, $(\Delta P_c)_{\max}$, must be larger than the total loop pressure drop ΔP_{loop} [6,16,17]; that is

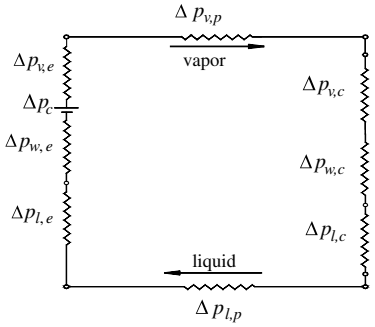

Fig. 1 Schematic diagram of a capillary head and pressure drop of a CPL.

$$(\Delta P_c)_{\max} \geq \Delta p_{\text{loop}} \tag{2}$$

The system pressure drop is schematically shown in Fig. 1. The total pressure loss ΔP_{loop} is achieved by the summation of the pressure drop of all the components in the loop, which can be written as follows:

$$\Delta p_{\text{loop}} = \Delta p_{vl} + \Delta p_{ll} + \Delta p_{w,e} + \Delta p_{w,c} + \Delta p_{\text{evap}} + \Delta p_{\text{cond}} + \Delta p_{\text{hydr}} \tag{3}$$

where Δp_{vv} is the pressure loss of the vapor line, Δp_{ll} is the pressure loss of the liquid line, $\Delta p_{w,e}$ is the pressure loss in the evaporator porous wick, $\Delta p_{w,c}$ is the pressure loss in the condenser porous wick, Δp_{evap} is the pressure loss during vaporization, Δp_{cond} is the pressure loss during condensation, and Δp_{hydr} is the hydrostatic pressure loss.

For the liquid and vapor, the pressure losses can be obtained according to the following equation:

$$\Delta P = f(Re) \cdot \frac{L}{D_h} \cdot \frac{\rho V^2}{2} \tag{4}$$

where L is the length of either liquid or vapor line, ρ is the density of liquid or vapor, D_{ll} is the hydraulic diameter of vapor or liquid line, and $f(Re)$ is the friction factor depending on the Reynolds number of liquid or vapor, which can be determined as follows [2]:

$$f(Re) = 64Re^{-1} \quad \text{if } Re < 2300 \tag{5}$$

$$f(Re) = 0.316Re^{-0.25} \quad \text{if } 2300 \leq Re \leq 20,000 \tag{6}$$

$$f(Re) = 0.184Re^{-0.2} \quad \text{if } Re > 20,000 \tag{7}$$

For the hydrostatic pressure loss

$$\Delta p_{\text{hydr}} = \rho_l g \Delta z \tag{8}$$

where Δz is the elevation difference between the free surface in the evaporator and condenser and g is the gravitational body force.

The pressure losses in the evaporator and the condenser porous wicks can be obtained by using Darcy's law, which is calculated from the following:

Pressure loss in the evaporator porous wick:

$$\Delta p_{w,e} = \frac{\mu_l \dot{m}_l L_{w,e}}{K_{w,e} A_{w,e} \rho_l} \tag{9}$$

Pressure loss in the condenser porous wick:

$$\Delta p_{w,c} = \frac{\mu_l \dot{m}_l L_{w,c}}{K_{w,c} A_{w,c} \rho_l} \tag{10}$$

The pressure losses during the phase change are given by the following:

Pressure loss during vaporization:

$$\Delta p_{\text{evap}} = \frac{\dot{m}_v}{A_{\text{evap}}} \sqrt{2\pi R_v T_v} \tag{11}$$

Pressure loss during condensation:

$$\Delta p_{\text{cond}} = \frac{\dot{m}_v}{A_{\text{cond}}} \sqrt{2\pi R_v T_v} \tag{12}$$

For the loop's mass flow rate:

$$\dot{m} = m_v = m_l = \frac{Q_{\text{total}}}{(h_{fg} + C_{pl}\Delta T_{\text{sub}})} \tag{13}$$

The velocity in liquid or the vapor line can be obtained as follows

$$V = \frac{\dot{m}}{\rho \cdot A} \tag{14}$$

where A is the flow aero of liquid or vapor line.

Besides satisfying the previous hydrodynamic relation, the CPL must meet energy balance requirements quoted as follows [14]:

$$Q_{\text{total}} = \dot{m}^2 \cdot \left(\frac{c_p \cdot h_{fg}}{A_c \cdot h_c}\right) + \dot{m} \cdot \left[h_{fg} + c_p \cdot T_s - \left(\frac{c_p \cdot Q_{\text{total}}}{A_c \cdot h_c}\right) - c_p \cdot T_{W,c}\right] \tag{15}$$

where Q_{total} is the total heat load applied on the evaporator, $\dot{m}$ is the mass flow rate of working fluid, h_{fg} is latent heat of liquid/vapor phase change, c_p is specific heat, T_s is the working fluid saturation temperature, and $T_{w,c}$ is the temperature of the condenser wall. A C-language program was created to design the CPL based on Eqs. (1–15) with different vapor/liquid line diameters which satisfy the pressure drop and energy balance relationship. Before analysis the evaporator and condenser sizes are selected with the design requirement. The size of the evaporator is 240×140 mm^2, the mesh number of stainless steel wire for the evaporator wick is 500, the size of the condenser is 260×140 mm^2, and the mesh number of the brass wire for the condenser wick is 250. Figure 2 shows the results of the analysis in a graph of different vapor/liquid line length vs the total heat load for flat-plate-type CPL. In the figure, the Dvap and Dliq represent the diameter of the vapor line and the liquid line, respectively. From the figure it can be observed that with the increasing of the line length, the maximum total heat load decreases. And the vapor line diameter has a great impact on the CPL maximum heat load.

With the design requirements, the structure parameters were selected from the above calculated results. The inner diameters of the liquid pipeline and the vapor pipeline are 4.5 and 8 mm, respectively. Based on the above-mentioned equations, according to its geometric

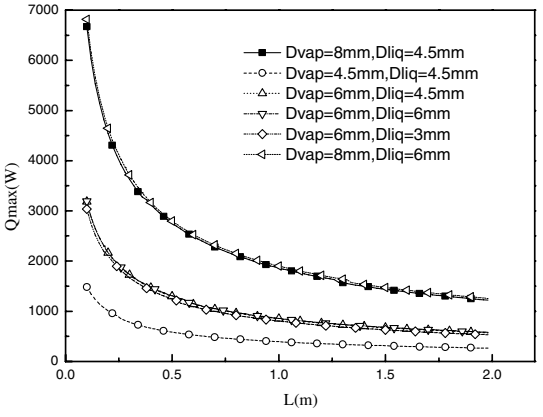

Fig. 2 Maximum transport distance based on the capillary pumping limit for flat-plate type of CPL.

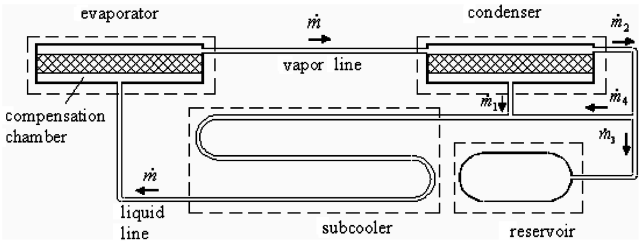

Fig. 3 Schematic diagram of a flat-plate-type CPL under investigation.

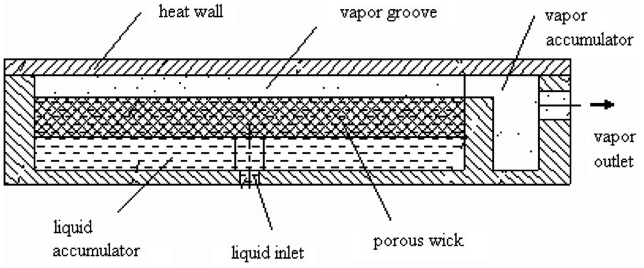

Fig. 4 Schematic of flat-plate type of evaporator.

characteristics, the total loop pressure losses of the calculated CPL under 400 W heat load is 246 Pa, the maximum capillary pumping force is 3376 Pa, and so the loop pressure losses are much less than the maximum capillary pumping force.

High-purity methanol (99.95%) was used as the working fluid in this research. To keep the system operation in low temperature, the system must work with a certain vacuum pressure.

Figure 3 schematically shows the conception model of new flat-plate CPL. For the CPL under investigation, both evaporator and condenser are designed as a flat-plate type with a porous wick, and a reservoir is used to control and adjust the operation temperature of the system. In addition, a subcooler is adopted to improve the returning fluid so that the working fluid can return to the evaporator efficiently. A plane evaporator with a cross channel for liquid supply was fabricated to reduce the probability of a dry-out point caused by strong evaporation in the case of high heat flux, and therefore to enhance the stability of the system. Figure 4 schematically shows the detailed structure of the evaporator. Also, a plane condenser with porous wick is designed, which has three ports for vapor-pipe inlet, liquid-pipe outlet, and adjusting pipe connected to the reservoir. The above design is significantly different from the traditional CPL. Because such a design can reduce the flow resistance, the fluid can be easily pressed into the reservoir, and it is expected that the startup performance and the adjustment capability of the present CPL system can be improved efficiently. The geometric characteristics of the CPL are presented in Table 1.

The CPL experimental system is schematically shown in Fig. 5. Thirty-five T-type thermocouples are used to monitor the temperature changes throughout the CPL, of which T1– T9 are used to monitor the evaporator temperature, T13–T15 and T17–T20 are used to monitor each condenser temperature, and T10 is fixed into the vapor line interior, so it can be seen as vaporizing temperature Tevp. Three pressure transducers are used to measure the pressures of the evaporator outlet, the condenser outlet, and the reservoir, respectively. A plane heater is used to simulate the heat load of the evaporator and an electrical heater is used to control the temperature in the reservoir. A 3 hp refrigeration system is chosen as the heat sink of the condenser.

All instruments are connected to a Keithley 2700 data acquisition system, where a computer monitors the temperature and pressure changes. Based on this experimental system, many operation performances such as reliability, temperature controlling and startup can be tested and verified. The experimental tests were divided into two parts. The first one is the startup test, in which CPL starts from room temperature conditions and reaches the steady state. In such a test, the time to reach the steady state is looked forward to be short, therefore the time to reach steady state was carefully observed. The

Table 1 The geometric characteristics of the new flat-plate type of CPL

	Evaporator	
Length, mm		240
Width, mm		140
	No.	25
Vapor groove	Width, mm	3
	High, mm	4
	Condenser	
Length, mm		260
Width, mm		140
	No.	25
Vapor groove	Width, mm	3
	High, mm	4
	Porous wick	
Permeability, m^2		6.524×10^{-12}
Porosity, %		59.41
	Reservoir	
Diameter, mm		60
Length, mm		120
	Vapor line	
Outer diameter, mm		10
Inner diameter, mm		8
	Liquid line	
Outer diameter, mm		6
Inner diameter, mm		4.5

second one is the heat load profile test, in which CPL is exposed to the power change applied to the capillary evaporator. In such a test, the CPL capability of following the changes of the heat load was examined.

III. Results and Discussion

A. Startup Test of CPL

The CPL startup tests were the most critical ones for evaluating the capillary evaporator reliability. Usually, there is a stronger tendency of depriming for capillary evaporators in normal CPL. However, in all tests conducted in the present experiments, this tendency was not observed. For startups at either small or large heat loads, the capillary evaporator is very reliable.

During the startup process the largest pressure difference in the system would occur. To clear the liquid of the vapor groove in a fully flooded CPL, the resulted vapor must displace the liquid from the vapor line and move it into the reservoir. The displacement results in a liquid mass flow rate described as follows:

$$\dot{m} = \frac{\rho_l}{\rho_v} \frac{\dot{Q}}{h_{fg}} \tag{16}$$

Owing to a large density difference of liquid and vapor, this mass flow rate is much greater than that achieved at steady state for the same power and results in temporarily large evaporator pressures, typically called pressure surge. The higher pressure is sustained as long as it takes to displace the liquid from the vapor line and condenser to the reservoir. In a traditional CPL there is only one fluid passage between the reservoir and the loop, so the flow resistance during startup is great and can result in startup difficulty, even failure. Aiming to improve the startup performance, we change both the component construction and the system configuration in present CPL. All startup tests succeed without pressure priming and liquid clearing of the vapor line, which demonstrates excellent startup performance. Figure 6 shows the startup test results at different heat loads. For each test, it could be observed that the capillary evaporator exhibits an excellent tendency of startup, and once the CPL starts up successfully, the system operates stably. For very low heat load ($Q = 50$ W, $Q = 100$ W), no obvious superheating was observed, and no distinct changing of the outlet temperature of the reservoir was verified. But for the heat load ($Q = 270$ W, $Q = 300$ W), higher superheating of the evaporator and larger temperature changing of the reservoir outlet were observed. The reason for these can be explained as follows. Because no pressure priming was conducted before startup in our CPL system, there may exist some vapor bubble or vapor space in the evaporator vapor channel, when the heat load was applied on the evaporator, and the liquid fluid can easily vaporize. And for $Q = 50$ W, the resulted vapor is small, and the mass flow rate is small according to Eq. (16), so the pressure surge is small, according to [18], and the superheating is low. But with high heat load ($Q = 270$ W, $Q = 300$ W) the vaporizing resulted vapor quantity becomes larger and the mass flow rate is increased, so a larger pressure surge takes place, which leads to a high pressure surge, and high superheating of the evaporator is observed. Excessive working fluid is expelled to the reservoir through the expelling passage of the condenser to maintain the normal operation, and so distinct reservoir outlet temperature changes are observed. The startup time for the small heat load ($Q = 50$ W, $Q = 100$ W) are longer than for large heat loads ($Q = 270$ W, $Q = 300$ W). It can be also observed that there is a high superheat with CPL startup with large heat loads ($Q = 270$ W, $Q = 300$ W). At small heat loads, because heat is slowly transferred to the working fluid, the menisci formation in the grooves takes more time; therefore it needs some time for the capillary force to generate. On the contrary, at large heat loads, the menisci form quickly and the capillary forces act faster.

The liquid compensation chamber is near to the capillary wick in the evaporator and integrates with the capillary evaporator to form one body design. Such a design makes the wick always be filled with liquid, so there is no need to preheat the reservoir for priming. Also, compared with traditional CPL, it can greatly reduce the flow

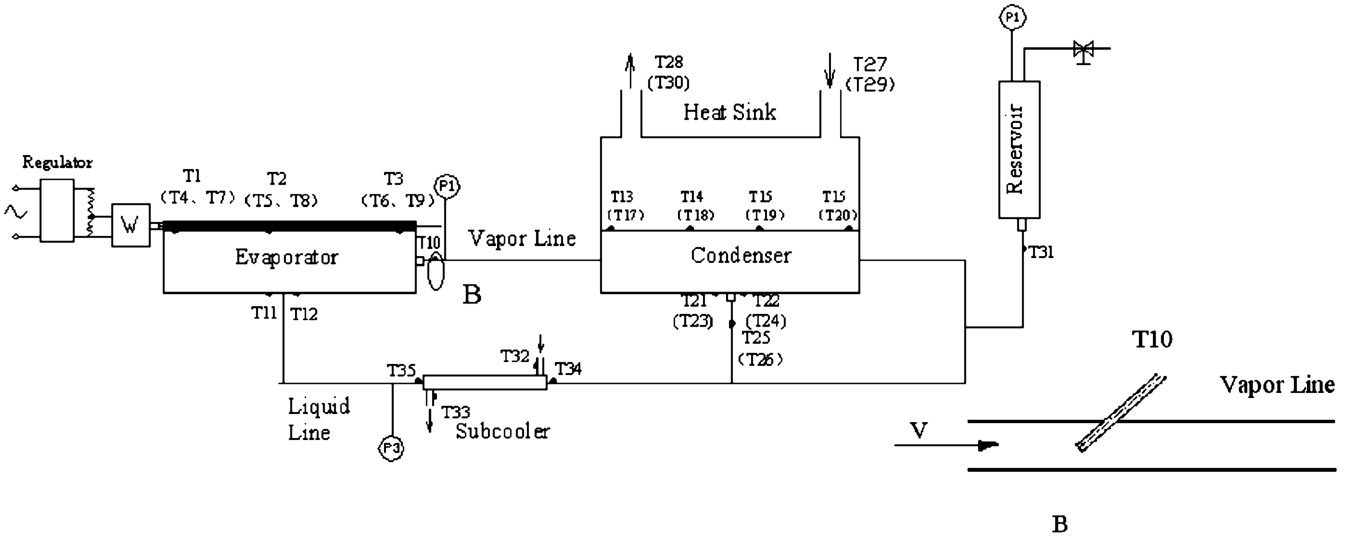

Fig. 5 Schematic diagram of CPL experimental setup.

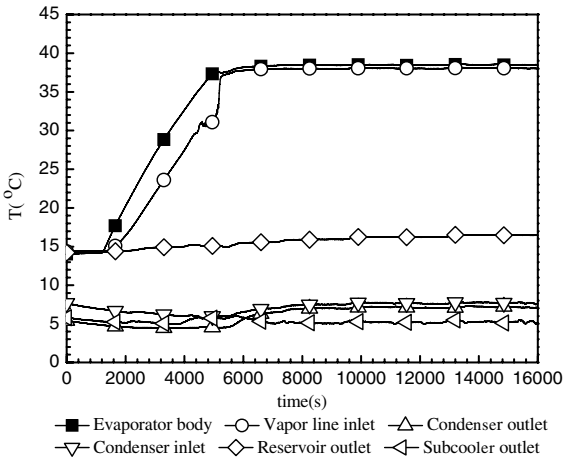

a) Q = 50 W

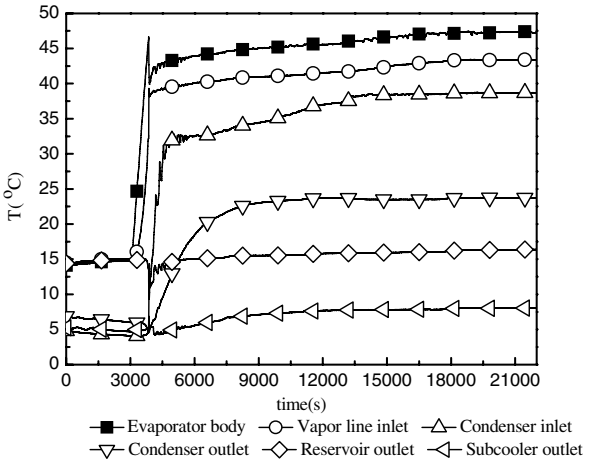

c) Q = 270 W

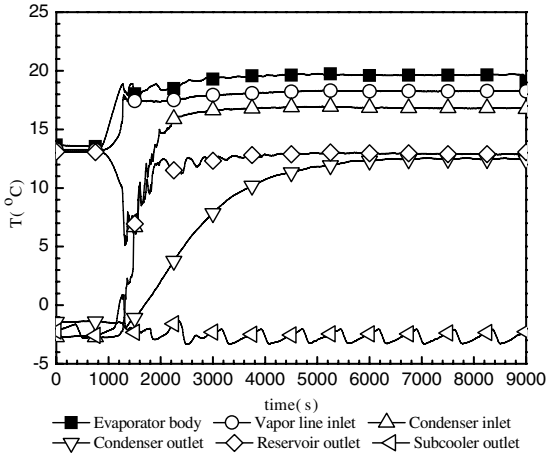

b) Q = 100 W

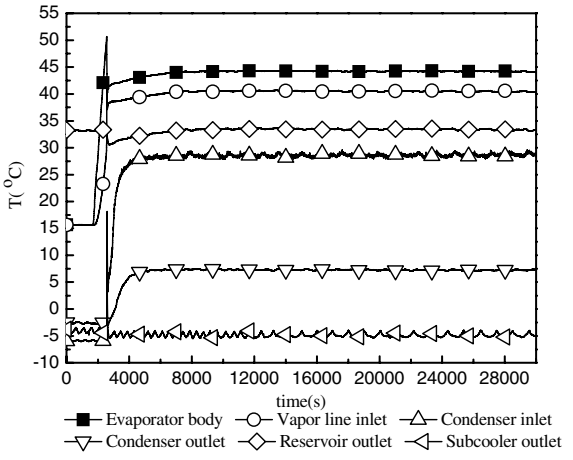

d) Q = 300 W

Fig. 6 CPL startup at different heat loads.

resistance between the condenser and the reservoir. As a result, the pressure surge of the liquid clearing of the vapor line can be significantly reduced, which enhances the possibility of startup success. The temperature distribution of the capillary evaporator is very homogeneous, without showing any tendency of overshooting, and the compensation chamber minimizes the possibility of evaporator depriming and the CPL failure.

B. Heat Load Test of CPL

To verify the proposed CPL thermal behavior at different heat loads applied to the capillary evaporator, the profile test was conducted. Such a test is very important to verify the CPL performance, for example, the performance of following different heat loads during continuous operation, the heat transfer performance when sudden power change appears. In addition, the aforementioned test is also important to observe the depriming potentiality. Figure 6 demonstrates the test results when two profiles were used. Figure 7a shows the temperature variation as the input power changes in the order of 100, 200, 100, and 200 W. Figure 7b shows the temperature variation as the input power changes in the order of 100, 200, 50, and 200 W. From Fig. 6, it can be observed that with the increasing of the heat load, the vapor temperature increases slightly and with the decreasing of the heat load, the vapor temperature also decreases slightly. The CPL responds quickly to the heat load variation; it just consumes a short time to reach the steady state again. From Fig. 7c, it is seen that although the heat load increases from 50 to 250 W, the system still can work stably, and the temperature increase is just only 4.3°C. The heat profile test demonstrates that present CPL is a robust design. The flat-plate capillary condenser has two out ports, one is from the condenser to the liquid line and another one is from the condenser to the reservoir. As mentioned previously, the fluid exchange between the reservoir and the CPL system depends on these two paths, which is a major difference between the present CPL and the traditional CPL. When the operation conditions change, for example, as shown in Fig. 3, when the heat load increases, to enlarge the condensation surface, some liquid marked as $\dot{m}_2$ is expelled out of the condenser. After $\dot{m}_2$ flows out of the condenser, it is divided into two sections, with one part flowing into the reservoir and another flowing to the liquid line. Such a design enlarges the condensation surface and ensures the sufficient liquid supply for the evaporator. When the heat load decreases, the fluid flow phenomena are similar to that at the case of heat load increasing, but the flow directions are opposite. The porous wick in the condenser generates a stable physical interface between the liquid and the vapor phases inside the CPL, which reduces or even eliminates the difficulties associated with the startup procedure and the pressure oscillations.

From Fig. 7 it can be observed that once the system starts up successfully, the evaporator temperature can remain stable, but the condenser inlet temperature presents some oscillation. There are 17 parallel fluid channels in our flat-plate condenser. When the vapor flows into the condenser, it can flow in all these channels, but the flow rates are not equal to each other in all channels. The condenser interface in all channels is different and changing. The test points of the condenser temperature lie in the centerline of the condenser along the flow direction, and so the temperature presents some oscillation. From Fig. 7b it can be observed that when the heat load is reduced from 200 to 50 W, the system presents unstable operation characteristics. The backconduction (heat transferred by conduction

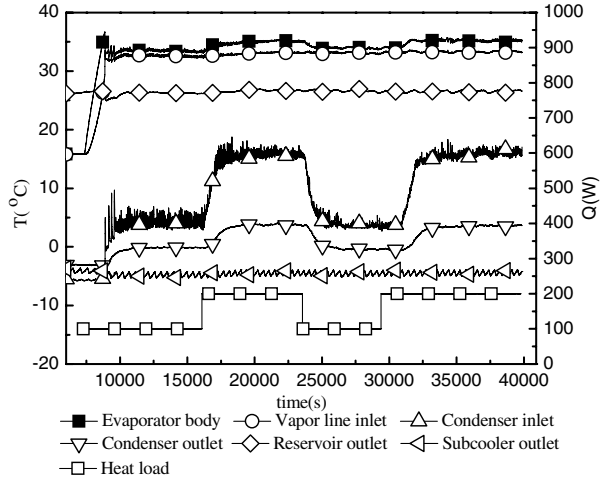

a) Q: 100-200-100-200 W

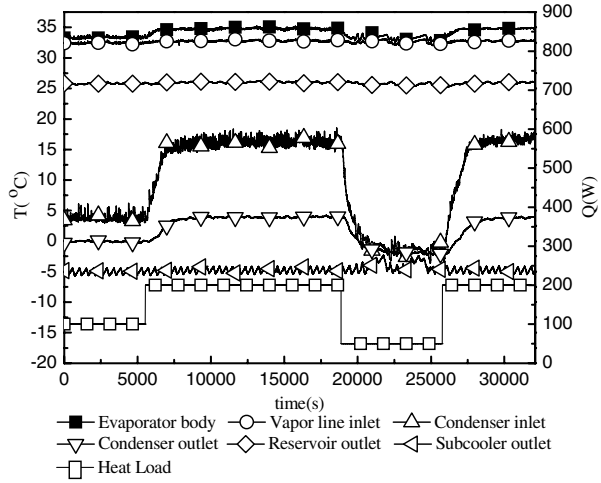

b) Q: 100-200-50-200 W

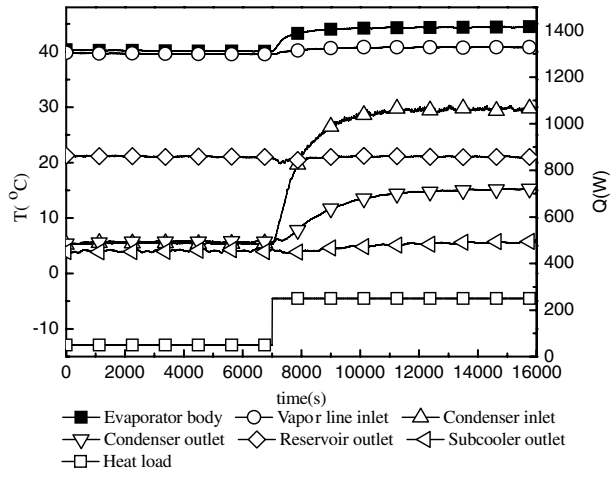

c) Q: 50-250 W

Fig. 7 CPL heat profile at different heat load variety.

from the heating surface to the liquid chamber through the evaporator wall or wick) for the flat-plate type of evaporation is obvious. With $Q = 200$ W the backconduction can be compensated through the large, cooler, return liquid flow rate. When heat flow is reduced to 50 W, the return liquid flow rate is also reduced and cannot compensate backconduction, and therefore the system cannot work stably.

From the observed results in the tests, the present CPL design shows good thermal behavior for both startup and heat load profile

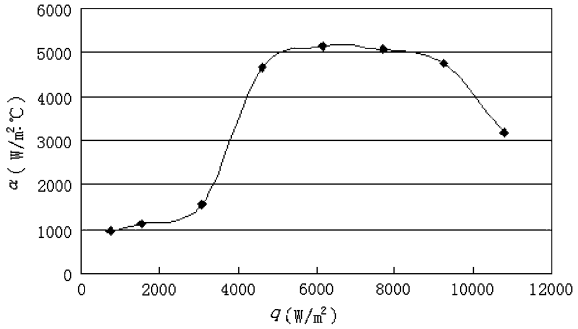

Fig. 8 Variations of the heat transfer coefficient vs the imposed heat flux of the CPL evaporator.

tests. The temperature of the capillary evaporator body is very stable without any overshooting at any time during its operation. The proposed system is proved to be able to operate for several hours continuously with very little variation under its operation conditions. If the same heat load is applied to the capillary evaporator, it is expected that the CPL can work continuously during its entire lifetime.

C. Heat Transfer Analysis of CPL Evaporator

The heat transfer coefficient of the evaporator can be defined as

$$a = \frac{q}{\Delta T} \tag{17}$$

where α is the heat transfer coefficient of the evaporator, Q is the heat load applied on the evaporator, and $\Delta T = T_e - T_{\text{vap}}$. T_e is the evaporator body temperature which can be obtained by averaging the temperature of T1 to T9, and T_{vap} is the temperature of the vapor line inlet.

Figure 8 shows the variation of the heat transfer coefficient with the heat flux applied on the evaporator. From the figure, it can be observed that with an increase of the imposed heat flux, the heat transfer coefficient increases to a maximum value and then decreases afterward. This phenomenon can be explained according to the visualized experiment of Zhao and Liao [14]. At a certain value of the imposed heat flux (for example, $Q = 1000$ W/m^2), nucleate boiling took place at the porous wick surface close to heated surface of the evaporator. The capillary force, which is derived from the meniscus formed at the liquid–vapor interface of the porous wick in the evaporator, drives the liquid fluid to flow, and as a result, a number of small dispersed bubbles were continuously generated. But these bubbles did not affect and combine with each other, so the heat transfer coefficient was small. As the imposed heat flux was increased further, both the numbers of the act of bubbles and the capillary force were increased. As a consequence, the heat transfer coefficient increased. When the imposed heat flux was further increased, the bubbles below the heated surface disappeared and there only a dry vapor film existed at the interface between the heated surface and the porous wick. In this situation, heat was transferred to the evaporating front within the porous structure via the vapor film. The lower thermal conductivity of the vapor film leads to a smaller heat transfer rate. This is why the heat transfer coefficient begins to drop beyond a certain value of heat flux. From the figure of the evaporator heat transfer capability a conclusion can be drawn that, although CPL shows good heat transfer capability during normal operation, its heat transfer capability is limited to some extent. When CPL is used in a high heat flux situation, the heat transfer capability limitation should be taken into account for insuring the CPL's normal operation.

IV. Conclusions

A new flat-plate-type CPL system is originally designed, fabricated, and tested in the present study. The testing results from the new type of CPL demonstrated the ability to start up without a

tedious pressure priming procedure and liquid clearing of the vapor line. It can keep a stable operation under severe operational conditions such as low load and sudden power step. Its adjusting performance is also improved compared with the normal CPL system. Some important directions for further work are miniaturizing the new flat-plate type of CPL and improving the high heat load performance.

References

[1] Stenger, F. J., "Experimental Feasibility Study of Water-Filled Capillary-Pumped Heat-Transfer Loops," NASA TM-X-1310, NASA Lewis Research Center, Cleveland, OH, 1966.

[2] Bazzo, E., and Riehl, R. R., "Operation Characteristics of a Small-Scale Capillary Pumped Loop," *Applied Thermal Engineering*, Vol. 23, No. 6, 2003, pp. 687–705. doi:10.1016/S1359-4311(03)00017-6

[3] LaClair, T. J., and Mudawar, I., "Thermal Transient in a Capillary Evaporator Prior to the Initiation of Boiling," *International Journal of Heat and Mass Transfer*, Vol. 43, No. 21, 2000, pp. 3937–3952. doi:10.1016/S0017-9310(00)00042-9

[4] Ottenstein, L., Butler, D., Ku, J., Cheung, K., Baldauff, R., and Hoang, T., "Flight Testing of the Capillary Pumped Loop 3 Experiment," *AIP Conference Proceedings*, Vol. 654, 2003, pp. 55–64. doi:10.1063/1.1541277

[5] Chen, P.-C., and Lin, W.-K., "The Application of Capillary Pumped Loop for Cooling of Electronic Components," *Applied Thermal Engineering*, Vol. 21, April 2001, pp. 1739–1754. doi:10.1016/S1359-4311(01)00045-X

[6] Butler, D., Ku, J., and Swanson, T., "Loop Heat Pipes and Capillary Pumped Loops—An Applications Perspective," *AIP Conference Proceedings*, Vol. 608, 2002, pp. 49–56. doi:10.1063/1.1449707

[7] Qu, Y., Peng, X. F., and Liu, T., "Flow and Heat Transfer Characteristics in the Porous Wick Condenser of CPL," *Science in China (Series E)*, Vol. 44, No. 5, 2006, pp. 499–506.

[8] Hoang, T., "Development of an Advanced Capillary Pumped Loop," Society of Automotive Engineers Paper 972315, 1997.

[9] Hoang, T., and Ku, J., "Hydrodynamic Aspect of Capillary Pumped Loop," Society of Automotive Engineers Paper 961435, 1996.

[10] Muraoka, I., Ramos, F. M., and Vlassov, V. V., "Experimental and Theoretical Investigation of Capillary Pumped Loop with a Porous Element in the Condenser," *International Journal of Heat and Mass Transfer*, Vol. 25, No. 8, 1998, pp. 1085–1094. doi:10.1016/S0735-1933(98)00099-2

[11] Ku, J., "Thermodynamic Aspects of Capillary Pumped Loop Operation," *6th AIAA/ASME Joint Thermophysics and Heat Transfer Conference*, AIAA, Washington, D.C., 20–23 June 1994.

[12] Huang, X. M., and Liu, W., "Numerical Study of the Phase-Change Heat Transfer in a Capillary Structure of CPL Evaporator," *Proceedings of the 13th International Heat Pipe Conference*, China Academy of Space Technology (CAST), Shangai, China, 2004.

[13] Huang, X. M., Liu, W., Nakayama, A., and Peng, S. W., "Modeling for Heat and Mass Transfer with Phase Change in Porous Wick of CPL Evaporator," *Heat and Mass Transfer*, Vol. 41, 2005, pp. 667–673. doi:10.1007/s00231-004-0609-2

[14] Liao, Q., and Zhao, T. S., "Evaporative Heat Transfer in a Capillary Structure Heated by a Grooved Block," *Journal of Thermophysics and Heat Transfer*, Vol. 13, No. 1, 1999, pp. 126–133.

[15] Figus, C., Bray, Y. L., and Bories, S., "Heat and Mass Transfer with Phase Change in a Porous Structure Partially Heated: Continuum Model and Pore Net Work Simulations," *International Journal of Heat and Mass Transfer*, Vol. 42, No. 14, 1999, pp. 2557–2569. doi:10.1016/S0017-9310(98)00342-1

[16] Hoang, T., Brown, M., Baldauff, R., and Cummings, S., "Development of a Two-Phase Capillary Pumped Heat Transport for Spacecraft Central Thermals Bus," *AIP Conference Proceedings*, Vol. 654, 2003, pp. 49–54. doi:10.1063/1.1541276

[17] Kirshberg, J., and Yerkes, K. L., "Demonstration of a Micro-CPL Based on MEMS Fabrication Technologies," AIAA Paper 3015, 2000.

[18] Ku, J., Hoang, T., Nguyen, T., and Yun, S., "Performance Tests of CAPL 2 Starter Pump Cold Plates," AIAA Paper 96-1837, 1996.